Sensors and Materials, Vol. 32, No. 4 (2020) 1411–1417
MYU Tokyo

S & M 2188

Optical and X-ray-induced Luminescence Properties of Calcium Phosphate of Transparent Ceramic Form

Takumi Kato,* Daisuke Nakauchi, Noriaki Kawaguchi, and Takayuki Yanagida

Nara Institute of Science and Technology (NAIST) 8916-5, Takayama-cho, Ikoma-shi, Nara 630-0192, Japan

(Received December 18, 2019; accepted March 2, 2020)

Keywords: transparent ceramic, calcium phosphate, luminescence properties, SPS

Undoped and Sb-doped calcium phosphate transparent ceramics were prepared by the spark plasma sintering technique, and their optical and X-ray-induced luminescence properties were investigated. Regarding their optical properties, the transmittance of the undoped transparent ceramic with a thickness of 1.05 mm was higher than 50% in the range of 500–2500 nm. The undoped calcium phosphate exhibited an emission peak at 450 nm due to excitons. On the other hand, the Sb-doped calcium phosphate showed a broad emission peak attributable to the $^3P_1$–$^1S_0$ transitions of Sb^{3+} ions around 500 nm in both PL and scintillation spectra. The obtained scintillation decay time constants of the 0.1% Sb-doped calcium phosphate were 1.2 and 7.9 μs. Glow peaks were detected at 90, 160, and 360 °C. The TSL intensity decreased with the increase in Sb concentration.

1. Introduction

Phosphor materials are often utilized in radiation detectors, and such materials can be classified into two types: scintillators and storage phosphors. Scintillators can instantly convert the energy of absorbed ionizing radiations into a large number of low-energy photons, and they have been widely used in fields requiring radiation detection, such as medicine,[1] security,[2] and environmental monitoring.[3] In general, the required properties of scintillators include high light yield, short decay time, and low afterglow. On the other hand, storage phosphors can temporally store the absorbed energy of ionizing radiations. The energy is stored in the form of carriers trapped at localized centers. The trapped electrons and holes can be released by heat or light stimulation with the emission of photons. The resultant luminescence is either thermally stimulated luminescence (TSL) or optically stimulated luminescence (OSL). Phosphors showing TSL or OSL have been mainly used in individual radiation monitoring[4–6] and imaging plates (IPs).[7,8] Generally, dose linearity, suitable sensitivity, slow fading, and energy response are required for TSL and OSL properties. Furthermore, if the aim is to measure the dose of radiation absorbed in the human body, it is preferred that the effective atomic number (Z_{eff}) of storage phosphors is close to that of the soft tissue (Z_{eff} = 7.13) from the viewpoint of bioequivalence; therefore, for dosimetry applications especially in protection dosimetry, it is desirable that storage phosphors are composed of light elements.

*Corresponding author: e-mail: kato.takumi.ki5@ms.naist.jp
https://doi.org/10.18494/SAM.2020.2742

ISSN 0914-4935

Regarding the forms of the phosphor materials utilized in radiation detectors, they can be categorized into three types: single crystal, opaque ceramic, and glass.[9–14] On the other hand, transparent ceramics have been attracting attention as a new material form of storage phosphors in recent years. In comparison with single crystals and opaque ceramics, transparent ceramics show outstanding TSL and OSL properties because of their high density of defect centers and transparency. The intensities of TSL and OSL generally depend on the density of defects acting as trapping centers, and ceramics contain more defects than single crystals. In addition, if the storage phosphor is transparent, we can detect TSL and OSL not only on the surface but also inside the materials.[15,16]

In this study, we synthesized undoped calcium phosphate transparent ceramics by the spark plasma sintering (SPS) technique and investigated their optical and X-ray-induced luminescence properties. Calcium phosphate is an essential component of bone and teeth. Since its effective atomic number is close to that of the human bone, calcium phosphate could be one of the candidate storage phosphors for dosimeters. Calcium phosphate can also be applied to scintillators for α-ray detection. On the other hand, the preparation method for transparent ceramics of calcium phosphate has already been reported.[17] However, there is no report on the optical and X-ray-induced luminescence properties of calcium phosphate transparent ceramics. Moreover, in this study, Sb-doped calcium phosphate transparent ceramics were synthesized by the SPS technique. It has long been known that Sb-doped calcium halophosphate, which was similar to calcium phosphate, showed an intense luminescence due to $^3P_1$–$^1S_0$ transitions of Sb^{3+} ions.[18]

2. Materials and Methods

Undoped and Sb-doped calcium phosphate transparent ceramic samples were prepared by the SPS technique using Sinter Land LabX-100. $Ca_3(PO_4)_2{\cdot}nH_2O$ (Kojundo Chemical Laboratory Corp., 99%) and Sb_2O_3 (Furuuchi Chemical Corp., 99.999%) powders were homogeneously mixed. 0.5 g of the mixture was loaded in a graphite die and held between two graphite punches. The sintering conditions used in various steps are shown in Fig. 1. First, the temperature was increased from 20 to 750 °C in 30 min and kept at this temperature for 10 min while applying a pressure of 6.5 MPa. Next, the temperature was increased from 750 to

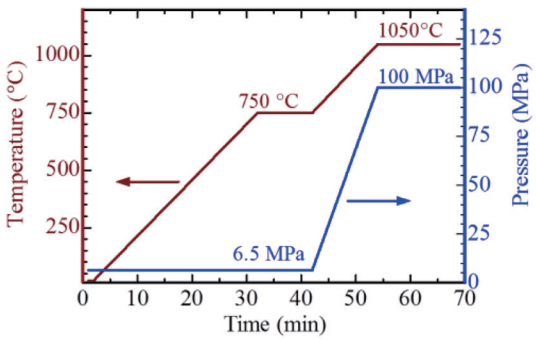

Fig. 1. (Color online) Sintering conditions used in the SPS technique.

1050 °C in 12 min while increasing the applied pressure to 100 MPa. Finally, the temperature was kept for 15 min while applying the pressure. After sintering, the wide surfaces of the obtained sample were mechanically polished using a polishing machine (MetaServ 250, BUEHLER). Scanning electron microscopy (SEM; JEOL JCM-6000plus) was used to observe backscattered electron images. The powder X-ray diffraction (XRD) pattern was measured using a diffractometer (MiniFlex600, Rigaku) over the 2θ range of 20–80°. The X-ray source is a conventional X-ray tube with a CuKα target operated at 40 kV and 15 mA.

To investigate optical properties, in-line transmission spectra were measured using a UV–visible near-infrared spectrophotometer V670 (JASCO Corporation). PL excitation and emission spectra were measured using a spectrofluorometer FP8600 (JASCO Corporation). Quantaurus-QY (C11347, Hamamatsu Photonics) was used to calculate quantum yields (*QY*s) under 250 nm excitation. Quantaurus-Tau (Hamamatsu Photonics) was used to measure PL decay profiles.

For X-ray-induced luminescence properties, scintillation spectra under X-ray irradiation were measured using our original setup.[19] The X-ray generator (XRB80N100/CB, Spellman) was equipped with an X-ray tube having a W anode target and a Be window. The X-ray tube was operated with a bias voltage of 60 kV and a tube current of 1.2 mA. In these analyses, scintillation photons emitted from the samples were led to a spectrometer unit equipped with a CCD (DU-420-BU2, Andor) and a monochromator (SR163, Shamrock) through an optical fiber to measure the spectra. Here, the detector was cooled to 188 K using a Peltier module to reduce the thermal noise. Scintillation decay curves were measured using an afterglow characterization system.[20] The excitation source used was a pulse X-ray tube, and the time resolution of the system was around 1 ns. The sensitivity of the photomultiplier tube (PMT) used was in the measurement range from 160 to 650 nm. TSL glow curves were measured using a commercial TSL reader (TL-2000, Nanogray)[21] after X-ray irradiations. The heating rate was fixed to 1 °C/s for all the glow curve measurements, and the measurement temperature range was from 50 to 490 °C.

3. Results and Discussion

Figure 2 shows photographs of the undoped and Sb-doped transparent ceramic samples. The thicknesses of the undoped, 0.01, 0.1, and 1.0% Sb-doped samples are 1.05, 1.01, 1.04, and 0.66 mm, respectively. The obtained samples except for the 1.0% Sb-doped sample are visually transparent, but the 1.0% Sb-doped sample strongly showed green luminescence under

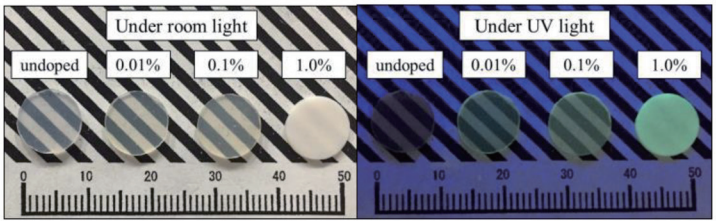

Fig. 2. (Color online) Photographs of undoped and Sb-doped transparent ceramic samples.

254 nm excitation. The density of the undoped sample measured by the Archimedes method was ~3.13 g/cm^3, which was equivalent to 99% of the theoretical density of $Ca_3(PO_4)_2$. Figure 3 shows SEM images of the polished surfaces of the (a) undoped and (b) 1.0% Sb-doped samples. From these measurements, the average grain size could not be confirmed, but the presence of some pores with a size of about 10 μm was confirmed in both samples. In contrast, it appeared that the surface of the 1.0% Sb-doped sample was rougher than that of the undoped sample. Figure 4 shows XRD patterns of the undoped and reference samples. No halo peaks could be observed in the measured XRD pattern of the undoped sample, indicating that the sample did not have an amorphous phase. Moreover, the XRD pattern of the sample agreed with that of $Ca_5HO_{13}P_3$, not $Ca_3O_8P_2$.

Figure 5 shows in-line transmittance spectra. The transmittance of the undoped sample was higher than 50% in the range of 500–2500 nm. In addition, the transmittance decreased with increasing Sb concentration. Absorption bands were detected around 1440, 2140, and 2600 nm for all the samples. These absorption bands are due to the host material; in particular, the absorption band around 2600 nm is attributed to a hydroxyl group.[22] This assignment is also supported by the measured XRD patterns. An absorption shorter than 250 nm is due to an optical absorption edge.[23]

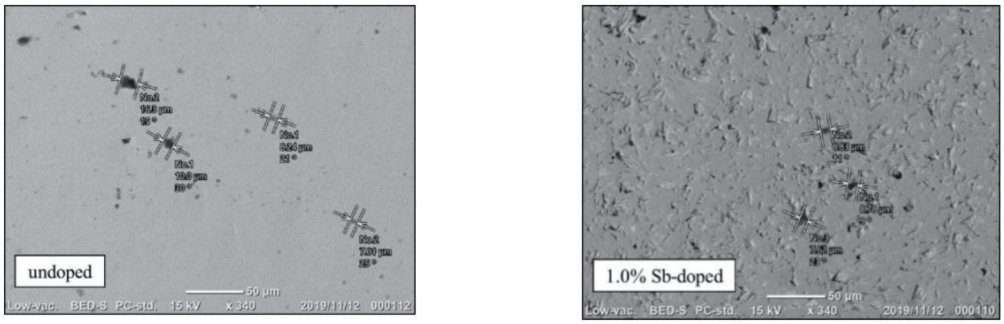

(a) (b)

Fig. 3. SEM images of polished surfaces of (a) undoped and (b) 1.0% Sb-doped samples.

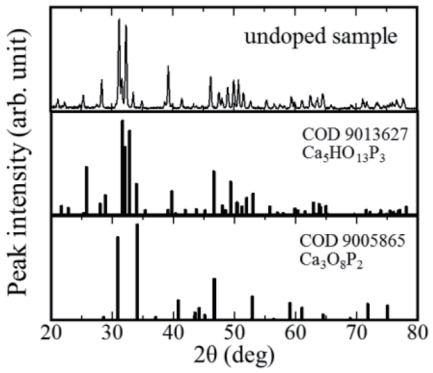

Fig. 4. XRD patterns of undoped and reference samples.

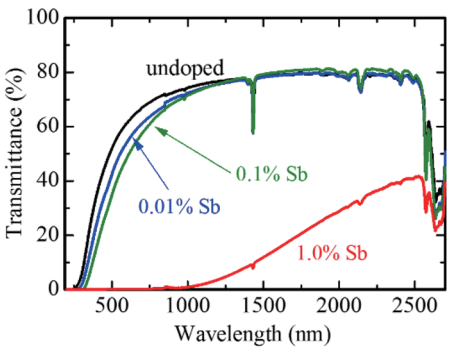

Fig. 5. (Color online) In-line transmittance spectra.

PL excitation and emission spectra of the undoped and Sb-doped samples are shown in Fig. 6. The undoped sample showed an emission peak at 450 nm under 230 nm excitation. This luminescence was considered to be caused by trapped excitons on the basis of a previous report that the undoped $Ca_3(PO_4)_2$ showed emission peaks from 300 to 550 nm due to trapped excitons.[24] On the other hand, the Sb-doped samples showed an emission peak at around 500 nm under 250 nm excitation. The luminescence from the Sb-doped samples was considered to be due to $^3P_1$–$^1S_0$ transitions of Sb^{3+} ions.[25] The *QY*s of the 0.01, 0.1, and 1.0% Sb-doped samples were 4.8, 4.8, and 6.3%, respectively. As a result, no concentration quenching was observed in the range from 0.01 to 1% in these samples.

Figure 7 shows PL decay curves of the undoped and 1.0% Sb-doped samples. The monitoring and excitation wavelengths were respectively 450 and 280 nm for the undoped sample, and 510 and 250 nm for the 1.0% Sb-doped sample. The PL decay curves of the undoped and Sb-doped samples were well approximated by one and two exponential decay functions, respectively. The derived decay time constant of the undoped sample was 391 ns. To the best of our knowledge, this is the first report on the decay time constant of the undoped calcium phosphate. The derived decay time constants of the 1.0% Sb-doped sample were 4.3 and 12.0 μs, and the other Sb-doped samples showed similar values. These values corresponded to the previously reported decay time constant and are attributable to $^3P_1$–$^1S_0$ transitions of Sb^{3+} ions.[26]

X-ray-induced scintillation spectra are shown in Fig. 8. The undoped sample exhibited an emission peak at 450 nm as well as PL, which was considered to be caused by excitons.[24] As the Sb concentration increased, the second emission peak was clearly detected at around 500 nm. This is due to $^3P_1$–$^1S_0$ transitions of Sb^{3+} ions as in the case of the assignment of PL. Figure 9 indicates the X-ray-induced scintillation decay time profiles of the undoped and 1.0% Sb-doped samples. The decay curves were approximated using one or two exponential decay functions. The obtained scintillation decay time constant of the undoped sample was 383 ns, which was consistent with the PL decay time constant. Moreover, the obtained scintillation decay time constants of the 0.1% Sb-doped sample were 1.2 and 7.9 μs, which roughly coincided with PL decay time constants. The decay time constants suggest that the origins of scintillation are the same as those of PL.

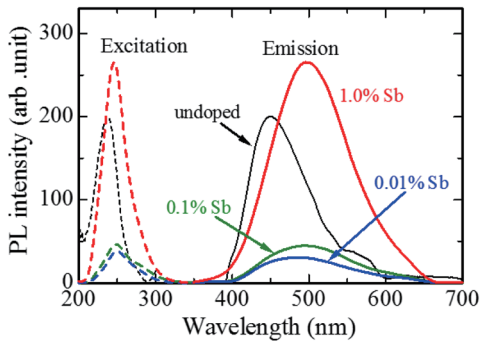

Fig. 6. (Color online) PL excitation and emission spectra of undoped and Sb-doped samples.

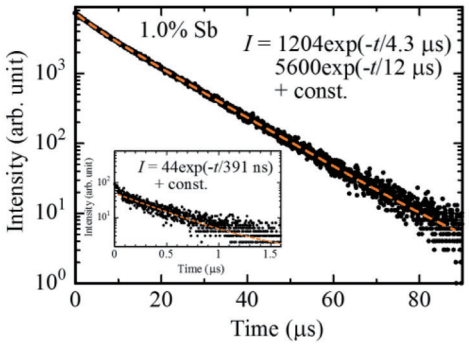

Fig. 7. (Color online) PL decay curve of 1.0% Sb-doped sample. The inset shows the PL decay curve of the undoped sample.

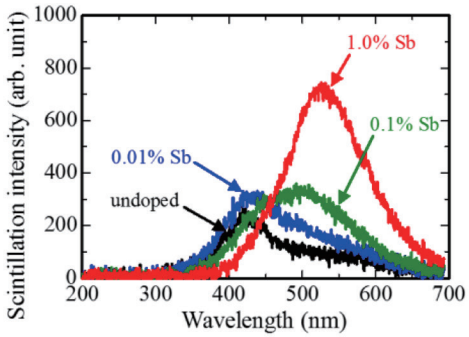

Fig. 8. (Color online) X-ray-induced scintillation spectra.

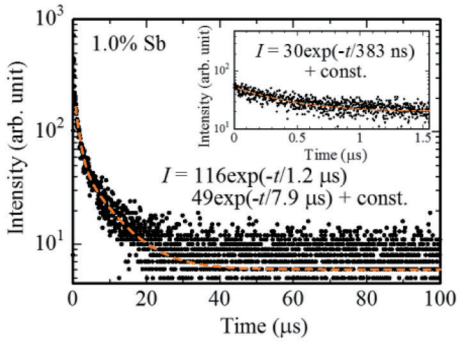

Fig. 9. (Color online) X-ray-induced scintillation decay curve of 1.0% Sb-doped sample. The inset shows the scintillation decay curve of the undoped sample.

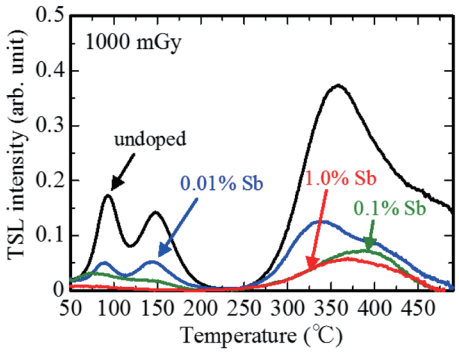

Fig. 10. (Color online) TSL glow curves obtained after samples irradiation at X-ray dose of 1000 mGy.

Figure 10 presents TSL glow curves obtained by subtracting the background after the samples were irradiated with an X-ray dose of 1000 mGy. The undoped sample showed three glow peaks at around 90, 160, and 360 °C, and the TSL intensities of all the glow peaks decreased with increasing Sb concentration. This result suggests that Sb doping suppressed the generation of trapping centers in calcium phosphate. Although these glow peaks were consistent with a previous report,[27] further discussion is required to clarify the origins of trapping centers.

4. Conclusions

We prepared undoped and Sb-doped calcium phosphate transparent ceramics by the SPS technique, and then investigated their optical and X-ray-induced luminescence properties. Because no halo peaks could be observed in its measured XRD pattern, the undoped sample did not have an amorphous phase. Moreover, the XRD pattern of the undoped sample agreed with that of $Ca_5HO_{13}P_3$, not $Ca_3O_8P_2$. The undoped calcium phosphate exhibited an emission peak attributable to excitons. In contrast, the Sb-doped calcium phosphate showed a broad emission peak attributable to the $^3P_1$–$^1S_0$ transitions of Sb^{3+} ions around 500 nm in both PL and scintillation spectra. In TSL glow curves, glow peaks were detected at 90, 160, and 360 °C.

Acknowledgments

This work was supported by Grants-in-Aid for Scientific Research A (17H01375) and B (18H03468 and 19H03533), and Young Scientists B (17K14911). The Cooperative Research Project of the Research Center for Biomedical Engineering of Iketani Foundation, Murata Foundation, and Nippon Sheet Glass Foundation is also acknowledged.

References

1 C. W. van Eijk: Nucl. Instrum. Methods Phys. Res., Sect. A **509** (2003) 17.
2 J. M. Hall, S. Asztalos, P. Biltoft, J. Church, M. A. Descalle, T. Luu, D. Manatt, G. Mauger, E. Norman, D. Petersen, J. Pruet, S. Prussin, and D. Slaughter: Nucl. Instrum. Methods Phys. Res., Sect. B **261** (2007) 337.
3 K. Watanabe, T. Yanagida, and K. Fukuda: Sens. Mater. **27** (2015) 269.
4 R. W. Christy, N. M. Johnson, and R. R. Wilbarg: J. Appl. Phys. **38** (1967) 2099.
5 Y. Hirata, K. Watanabe, S. Yoshihashi, A. Uritani, Y. Koba, N. Matsufuji, T. Yanagida, T. Toshito, and K. Fukuda: Sens. Mater. **29** (2017) 1455.
6 G. Okada, T. Kato, D. Nakauchi, K. Fukuda, and T. Yanagida: Sens. Mater. **28** (2016) 897.
7 H. Nanto, A. Nishimura, M. Kuroda, Y. Takei, and Y. Nakano: Nucl. Instrum. Methods Phys. Res., Sect. A **580** (2007) 278.
8 N. M. Winch, A. Edgar, and C. M. Bartle: Nucl. Insttum. Methods Phys. Res., Sect. A **763** (2014) 394.
9 N. Kawaguchi, H. Kimura, M. Akatsuka, G. Okada, N. Kawano, K. Fukuda, and T. Yanagida: Sens. Mater. **30** (2018) 1585.
10 T. Yanagida, H. Masai, M. Koshimizu, and N. Kawaguchi: Sens. Mater. **31** (2019) 1225.
11 Y. Koba, R. Shimomura, W. Chang, K. Shinsho, S. Yanagisawa, G. Wakabayashi, K. Matsumoto, H. Ushiba, and T. Ando: Sens. Mater. **30** (2018) 1599.
12 K. Shinsho, D. Maruyama, S. Yanagisawa, Y. Koba, M. Kakuta, K. Matsumoto, H. Ushiba, and T. Andoh: Sens. Mater. **30** (2018) 1591.
13 N. Kawano, N. Kawaguchi, G. Okada, Y. Fujimoto, and T. Yanagida: Sens. Mater. **30** (2018) 1539.
14 D. Shiratori, Y. Isokawa, N. Kawaguchi, and T. Yanagida: Sens. Mater. **31** (2019) 1281.
15 H. Kimura, T. Kato, D. Nakauchi, M. Koshimizu, N. Kawaguchi, and T. Yanagida: Sens. Mater. **31** (2019) 1265.
16 H. Kimura, F. Nakamura, T. Kato, D. Nakauchi, G. Okada, N. Kawaguchi, and T. Yanagida: Sens. Mater. **30** (2018) 1555.
17 D. Kawagoe, K. Ioku, H. Fujimori, and S. Goto: J. Ceram. Soc. Jpn. **112** (2004) 462.
18 F. Wen, X. Zhao, H. Ding, H. Huo, and J. Chen: J. Mater. Chem. **12** (2002) 3761.
19 T. Yanagida, K. Kamada, Y. Fujimoto, H. Yagi, and T. Yanagitani: Opt. Mater. **35** (2013) 2480.
20 T. Yanagida, Y. Fujimoto, T. Ito, K. Uchiyama, and K. Mori: Appl. Phys. Express. **7** (2014) 5.
21 T. Yanagida, Y. Fujimoto, N. Kawaguchi, and S. Yanagida: J. Ceram. Soc. Jpn. **121** (2013) 988.
22 S. Chen, Y. Wu, and Y. Yang: J. Am. Ceram. Soc. **96** (2013) 1694.
23 P. P. Mokoena, M. Gohain, V. Kumar, B. C. B. Bezuidenhoudt, H. C. Swart, and O. M. Ntwaeaborwa: J. Alloys Compd. **595** (2014) 33.
24 A. Lecointre, A. Bessière, B. Viana, R. A. Benhamou, and D. Gourier: Radiat. Meas. **45** (2010) 273.
25 F. Wen, J. Chen, J. Moon, H. Kim, J. Niu, and W. Li: J. Solid State Chem. **177** (2004) 3114.
26 M. Neff, V. Romano, and W. Lüthy: Opt. Mater. **33** (2010) 1.
27 K. Mizuguchi and Y. Fukuda: Radiat. Prot. Dosimetry. **84** (1999) 301.